Characteristics of silicon nitride deposited by VHF (162 MHz)-plasma enhanced chemical vapor deposition using a multi-tile push–pull plasma source

2016 J. Phys. D: Appl. Phys. 49 395201

(http://iopscience.iop.org/0022-3727/49/39/395201)

IOP Publishing Journal of Physics D: Applied Physics
J. Phys. D: Appl. Phys. **49** (2016) 395201 (8pp) doi:10.1088/0022-3727/49/39/395201

Characteristics of silicon nitride deposited by VHF (162 MHz)-plasma enhanced chemical vapor deposition using a multi-tile push–pull plasma source

Ki Seok Kim[1], Nishant Sirse[2], Ki Hyun Kim[1], Albert Rogers Ellingboe[2], Kyong Nam Kim[3] and Geun Young Yeom[1,4]

[1] School of Advanced Materials Science and Engineering, Sungkyunkwan University, 2066 Seobu-ro, Jangan-gu, Suwon-si, Gyeonggi-do 16419, Korea
[2] Plasma Research Laboratory, School of Physical Sciences, Dublin City University, Dublin 9, Ireland
[3] School of Advanced Materials Science and Engineering, Daejeon University, Yongun-dong, Dong-gu, Daejeon 34520, Korea
[4] SKKU Advanced Institute of Nano Technology (SAINT), Sungkyunkwan University, 2066 Seobu-ro, Jangan-gu, Suwon-si, Gyeonggi-do 16419, Korea

E-mail: knam1004@dju.kr and gyyeom@skku.edu

Received 31 May 2016, revised 17 July 2016
Accepted for publication 8 August 2016
Published 2 September 2016

Abstract

To prevent moisture and oxygen permeation into flexible organic electronic devices formed on substrates, the deposition of an inorganic diffusion barrier material such as SiN_x is important for thin film encapsulation. In this study, by a very high frequency (162 MHz) plasma-enhanced chemical vapor deposition (VHF-PECVD) using a multi-tile push–pull plasma source, SiN_x layers were deposited with a gas mixture of NH_3/SiH_4 with/without N_2 and the characteristics of the plasma and the deposited SiN_x film as the thin film barrier were investigated. Compared to a lower frequency (60 MHz) plasma, the VHF (162 MHz) multi-tile push–pull plasma showed a lower electron temperature, a higher vibrational temperature, and higher N_2 dissociation for an N_2 plasma. When a SiN_x layer was deposited with a mixture of NH_3/SiH_4 with N_2 at a low temperature of 100 °C, a stoichiometric amorphous Si_3N_4 layer with very low Si–H bonding could be deposited. The 300 nm thick SiN_x film exhibited a low water vapor transmission rate of 1.18×10^{-4} g $(m^2 \cdot d)^{-1}$, in addition to an optical transmittance of higher than 90%.

Keywords: silicon nitride, very high frequency, multi-tile push–pull, vibrational temperature

(Some figures may appear in colour only in the online journal)

1. Introduction

Organic electronic materials used for printed electronics and flexible organic light emitting diode (OLED) displays are highly vulnerable to moisture and oxygen. Accordingly, thin film encapsulation that prevents moisture and oxygen permeation into flexible substrates represents one of the most important technologies for next generation flexible electronic device fabrication. Especially, dense and stoichiometric thin film deposition at a lower temperature serves as the main key, not only to prevent the deformation of the flexible substrate, but also to prevent the degradation of organic devices deposited on the substrate [1–3].

For thin film encapsulation, silicon nitride (Si_3N_4) represents the most common material used for flexible polymer substrates, due to excellent properties, such as high transparency in the visible and infrared regions, thermal stability, abrasion resistance, and corrosion resistance [2, 4, 5]. However,

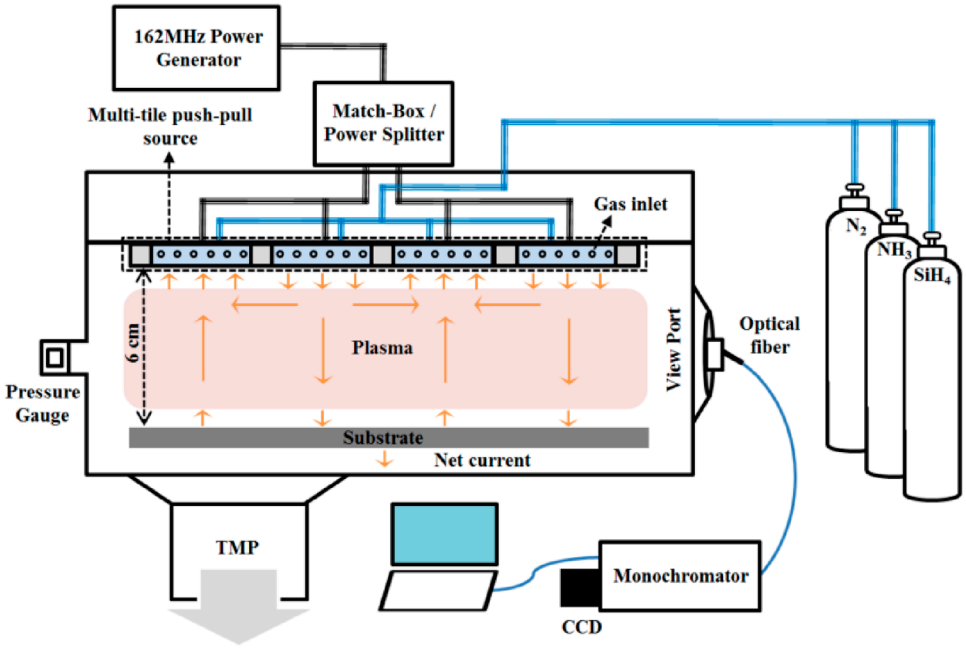

Figure 1. Schematic diagram of the VHF (162 MHz)-PECVD system with a multi-tile push–pull plasma source.

deposition of a film with high stoichiometry (chemical composition close to amorphous Si_3N_4), high density, good adhesion, and good uniformity on flexible substrates at a low temperature presents difficulties. In an attempt to overcome such challenges, many research investigations have employed various methods (e.g. physical vapor deposition (PVD), atomic layer deposition (ALD), plasma-enhanced CVD (PECVD), etc…). Recently, the ALD technique has attracted much attention by researchers, due to an almost defect-free deposition of material with superior step coverage [6–8]. A very low water vapor transmission rate (WVTR) (under 10^{-5} g $(m^2 \cdot d)^{-1}$) has been reported by decoupling the defects using a consecutive organic/inorganic hybrid layer structure [9–11]. However, ALD offers an extremely low (<1 nm min^{-1}) deposition rate, while limiting the range of producible materials [9, 11]. Alternatively, PECVD represents the most widely investigated technique allowing high throughput, due to its relatively high deposition rate over a large area. However, PECVD presents damage issues by ion bombardment during the deposition (on the substrate and/or on the organic device surface), as well as issues with porosity/less conformal step coverage of the film compared to that deposited by ALD, requiring resolution for effective moisture protection [12–14].

Recently, very high frequency PECVD (VHF-PECVD) technologies (operated at frequencies higher than 30 MHz) have been investigated for high quality and high rate thin film deposition, due to higher generation rates of radicals, lower ion bombardment energy, higher electron density (n_e), and lower electron temperature (T_e) than conventional high frequency (HF; 3–30 MHz; generally 13.56 MHz) PECVD [15–22]. However, the use of VHF instead of HF tends to increase deposition uniformity problems, due to the plasma non-uniformities caused by standing wave effects [23, 24].

Previously, a multi-tile push–pull plasma source has been investigated for VHF plasmas, in order to solve the issue of standing wave effects and to remove problems related to matching during operation [25]. In this study, we used a VHF (162 MHz)-PECVD equipped with a similar multi-tile push–pull plasma source for the deposition of a SiN_x layer, and we investigated the characteristics of the VHF plasma, as well as those of SiN_x films deposited by the plasma source as a thin film encapsulation layer. A highly-optically transparent SiN_x film with a chemical composition similar to stoichiometric amorphous Si_3N_4 [26–28] could be deposited with a gas mixture of NH_3/SiN_4 diluted in N_2 at low temperature of 100 °C, being compatible with most polymer substrates [29, 30]. Especially, using this plasma source, a very low WVTR of 1.18×10^{-4} g $(m^2 \cdot d)^{-1}$ could be obtained by depositing a 300 nm thick SiN_x film.

2. Experimental procedure

The schematic diagram of the VHF (162 MHz) PECVD system with the multi-tile push–pull plasma source is shown in figure 1. The multi-tile push–pull plasma source used in this study was composed of 8 sets (one set: two adjacent electrodes forming one push electrode and one pull electrode) of 300 mm × 58 mm electrode tiles, while these tiles were arranged on the top planar electrode surface similar to a checker board. Each set of tile electrodes was connected to the matcher/power splitter and was equally powered by inductive coupling to the radio frequency (rf) power at the power splitter. The two push–pull electrodes were not connected to the ground, allowing the current to flow between the push–pull electrodes without flowing to the substrate. On each tile electrode, 126 gas holes of 0.5 mm diameter were formed as

a shower head to distribute a gas mixture uniformly on the substrate. The substrate was located 6 cm below the multi-tile electrode and was heated using a heater. Additional details of the VHF (162 MHz) PECVD system with the multi-tile push–pull plasma source can be found elsewhere [25].

Soda-lime glass and polyethylene terephthalate (PET) were used as substrates, while depositing SiN_x on the substrates with gas mixtures composed of N_2, NH_3, and SiH_4. We used two different gas mixtures of NH_3 (150 sccm)/SiH_4 (50 sccm) = 3:1 and NH_3 (150 sccm)/SiH_4 (50 sccm)/N_2 (200 sccm) = 3:1:4 (i.e. with and without N_2) for the deposition of SiN_x film at 50 mTorr, while keeping the substrate temperature at 100 °C.

The characteristics of the plasmas (e.g. electron temperature (T_e), vibrational temperature (T_v), and N_2 gas dissociation (N/N_2)) were measured by optical emission spectroscopy (OES, Andor istar DH 734 with a spectrometer consisting of a grating monochromator and an intensified charge coupled device) using a view port (quartz window) located on the chamber wall, as shown in figure 1. To investigate the effect of higher rf frequency on the plasma characteristics, the plasma characteristics of 60 MHz capacitively coupled plasma (CCP) were also measured using the OES, comparing the data with those obtained with the 162 MHz multi-tile push–pull plasma source under similar process conditions.

For determining electron and vibrational temperatures, only N_2 gas was used. As reported in the literature, for the N_2 plasma, if the electron energy distribution function of the plasma is a Maxwell–Boltzmann distribution and if the concerned radiative states are caused by direct excitation by electron collisions from the N_2 ground state (i.e. relatively low pressure operation), equation (1) can be determined using the optical band head emission ratio of N_2^+ (B,0-X,0) transition at 391.4 nm and N_2 (C,2-B,5) transition at 394.3 nm [31, 32].

$$T_e(\mathrm{eV}) = \mathrm{fn}\left[\frac{I(391.4\,\mathrm{nm})}{I(394.3\,\mathrm{nm})}\right]. \quad (1)$$

The graph reflecting the dependence between the peak ratios and the electron temperature can be found elsewhere [31]. For the vibrational temperature (T_v) of the N_2 plasma, by assuming that the population density of the vibrational excited state was described by a Boltzmann distribution [31], it could also be determined by measuring the radiative transition intensities between the C and B electronic states of N_2 ($N_2(C^3\Pi_u) \rightarrow N_2(B^3\Pi_g) + I(v' - v'')$) and from the inverse of the slope ($1/kT_v$) of the flowing Boltzmann equation (2);

$$\ln\left[\frac{I(v' - v'')}{A(v' - v'')} \cdot \lambda\right] = -\frac{E_v - E_0}{kT_v} + \mathrm{const.} \quad (2)$$

Here, $I(v' - v'')$ was the measured optical emission intensity between the $C^3\Pi_u$ and $B^3\Pi_g$ electronic states with vibrational quantum numbers v' and v'', respectively, while $A(v' - v'')$ was the spontaneous emission probability that could be found elsewhere [33]. $E_v - E_0$ represented the vibrational energy difference of the excited molecule, while T_v was the effective vibrational temperature in the $C^3\Pi_u$ state. When the emitting electronic states and the ground level electronic states are in local thermodynamic equilibrium, the temperature determined from the excited state represents the temperature of the ground state molecules. Furthermore, in the case of second positive system of $N_2(C^3\Pi_u)$, the N_2 emitting electronic state is primarily populated by the direct transition from the ground state and, therefore, provides good approximation of the ground state vibrational temperature. To obtain T_v, optical emission intensities from 365 to 382 nm for vibrational quantum number differences $v' - v'' = 2$ (0–2 at 380.4 nm, 1–3 at 375.4 nm, 2–4 at 370.9 nm, and 3–5 at 367.0 nm) were chosen to determine the vibrational temperature. A detailed explanation on the T_v calculation can be found elsewhere [31].

The chemical binding states of the SiN_x were measured by Fourier transform infrared spectroscopy (FTIR, Bruker IFS-66/S, TENSOR27) for the wave number range from 500 to 4000 cm^{-1} with increment of 1.9 cm^{-1}, while the atomic composition of the SiN_x was measured using x-ray photoelectron spectroscopy (XPS, MultiLab 2000, Thermo VG, Mg Kα source) after calibrating the peak energies using the C1s peak at 284.5 eV. The optical transmittance of the SiN_x deposited on the glass substrate was measured by ultraviolet–visible–near infrared (UV–Vis NIR) spectroscopy (Shimadzu, 3600). For the WVTR of the SiN_x encapsulation layer, the Ca test (measuring the change of electrical conductance with time by the transmitted moisture) was carried out at the accelerating condition of 85 °C and 85% relative humidity (RH). For the Ca test, a Ca layer was deposited on a glass substrate (300 nm Ca layer with an area of 1 (l) × 1.4 (b) cm^2), and the Ca layer was connected to two aluminum electrodes (150 nm), and then, it was covered with the 300 nm thick SiN_x layer for encapsulation. The formula for the WVTR measurement by the Ca test is as follows;

$$\mathrm{WVTR}\ (\mathrm{g\,(m^2{\cdot}d)^{-1}}) = \frac{\text{Total grams of } H_2O}{(l \times b)} \times \frac{10\,000\ \mathrm{cm^2}}{\mathrm{m^2}} \times \frac{24\ \mathrm{h}}{\mathrm{day}} \times \frac{1}{t}. \quad (3)$$

WVTR was calculated by equation (3), where l, b and t are the length of Ca, the width of Ca, and the complete Ca oxidation time, respectively. Total gram of H_2O was 5.859×10^{-5}.

3. Results and discussion

Figure 2 shows the optical band head intensity ratios of N_2^+ (391.4 nm)/N_2 (394.3 nm) measured using OES, and the electron temperature (T_e) estimated using the intensity ratios of N_2 plasmas as a function of different rf power densities (235–1410 mW cm^{-2}) at different operating pressures (50–250 mTorr) for the 162 MHz multi-tile push–pull plasma source. As a comparison, we also measured the ratio of N_2^+ (391.4 nm)/N_2 (394.3 nm) and T_e of a conventional CCP operated at 60 MHz as a function of similar rf power densities with 50 mTorr N_2.

As shown in figure 2, the T_e of the 162 MHz multi-tile push–pull plasma source increased with the increase of rf power density and decreased with the increase of working pressure, similar to typical CCP sources (but with T_e generally

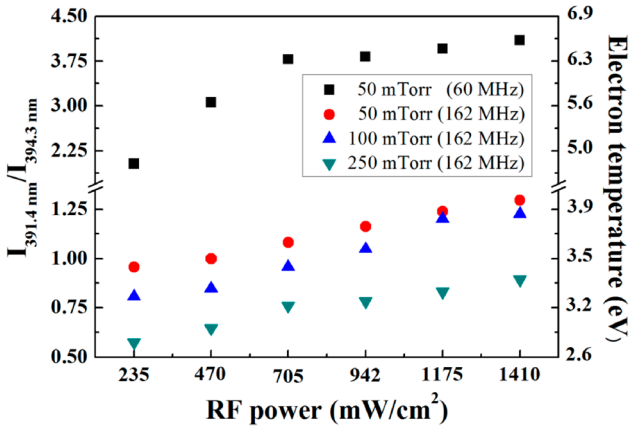

Figure 2. Optical band head intensity ratios of N_2^+ (391.4 nm)/N_2 (394.3 nm) measured using OES, and the electron temperature (T_e) estimated using the intensity ratios of N_2 plasmas as a function of different rf power densities (235–1410 mW cm^{-2}) for different operating pressures (50–250 mTorr) for the 162 MHz multi-tile push–pull plasma source. As a comparison, those of a conventional CCP operated at 60 MHz as a function of similar rf power densities with 50 mTorr N_2 were also measured.

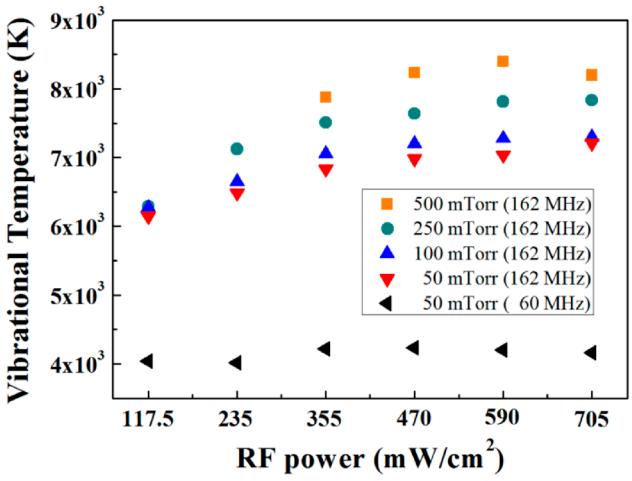

Figure 3. Vibrational temperatures of the N_2 plasmas measured as a function of different rf power densities (117.5–705 mW cm^{-2}) at different operating pressures (50–500 mTorr) for the 162 MHz multi-tile push–pull plasma source. The vibrational temperatures (T_v) of a conventional CCP operated at 60 MHz as a function of similar rf power densities with 50 mTorr N_2 were also measured.

lower than 3.9 eV). Previous studies have shown that the use of higher frequency for the CCP source (instead of conventional lower power frequency of 13.56 MHz) not only increased the plasma density (n_e), but also decreased T_e at the same rf power and operating pressure [18–20]. Similarly, in our experiment, the T_e of the N_2 plasma operated with a conventional CCP source at 60 MHz was generally higher than the T_e of an N_2 plasma operated with the 162 MHz plasma source at similar rf power densities and at the same N_2 pressure. For example, at 705 mW cm^{-2} of rf power density and 50 mTorr N_2 pressure, the 60 MHz CCP source showed about 6.34 eV of T_e, while the 162 MHz multi-tile push–pull plasma source showed about 3.55 eV. (The effective electron temperature measured by OES technique represent group of electrons with energies above the excitation and ionization thresholds, therefore, a higher electron temperature than expected by an electrostatic probe could be obtained. Similar electron temperature, 6 eV, is measured previously in a 60 MHz CCP by OES [34].)

For the multi-tile push–pull type source, in addition to the lower T_e due to the higher operating frequency compared to the conventional CCP source, the voltages induced on the tile electrodes were floated and the current flowed horizontally without flowing through the substrate, due to the relative voltage difference between two parallel tile electrodes. Therefore, a reduction in damage to the substrate was expected not only due to the lower T_e, but also due to the lack of current flow to the substrate. In addition, for conventional CCP sources, the use of higher VHF for the plasma processing increased the plasma non-uniformity, due to the standing wave problem formed on the electrode surface caused by the shorter wavelength at the higher operating frequency; therefore, the use of higher VHF for large area plasma processing is generally prevented, despite obtaining higher plasma density and lower T_e at higher operating rf. However, in the case of the multi-tile push–pull plasma source, the standing wave problems could be effectively eliminated for operation at higher VHF frequencies, due to the use of small parallel multi-tile electrodes, proving more applicable to large area plasma processing [25].

Figure 3 shows the vibrational temperatures (T_v) of the N_2 plasmas measured as a function of different rf power densities (117.5–705 mW cm^{-2}) at different operating pressures (50–500 mTorr) for the 162 MHz multi-tile push–pull plasma source. Also, for comparison, we measured the vibrational temperatures (T_v) of a CCP operated at 60 MHz as a function of similar rf power densities with 50 mTorr N_2.

The increase of both rf power and operating pressure increased the T_v slightly, indicating the increase of chemical reactivity of N_2 molecules. Previous research also showed that the T_v increased with the increase of rf power due to the increased electron density, as well as with the increase of operating pressure due to the decrease of T_e at the higher operating pressure [35]. (The number of vibrational excited molecules, i.e. T_v, was proportional to the electron density and vibrational excitation rate coefficient. Previous research showed that the vibrational excitation rate coefficient increased with the decrease of T_e, until around 3 eV for N_2 plasmas [35]. As shown in figure 2, the increase of operating pressure from 50 to 250 mTorr at 705 mW cm^{-2} decreased the electron temperature from ~3.6 to ~3.2 eV; therefore, we believe that the increased operating pressure increased the T_v by increasing the vibrational excitation rate coefficient.) At the similar rf power densities and at 50 mTorr, the T_v was lower for the 60 MHz CCP than for that of the 162 MHz multi-tile push–pull plasma. For example, at 705 mW cm^{-2} and 50 mTorr, the 162 MHz multi push–pull plasma source showed 7210 °K, while the 60 MHz CCP source exhibited 4160 °K, possibly due to the higher T_e for the 60 MHz CCP. Other previous research reported a lower T_v of 3000 ± 500 °K for a conventional 13.56 MHz CCP, supporting our belief of obtaining a higher T_v at a higher operating frequency [36, 37].

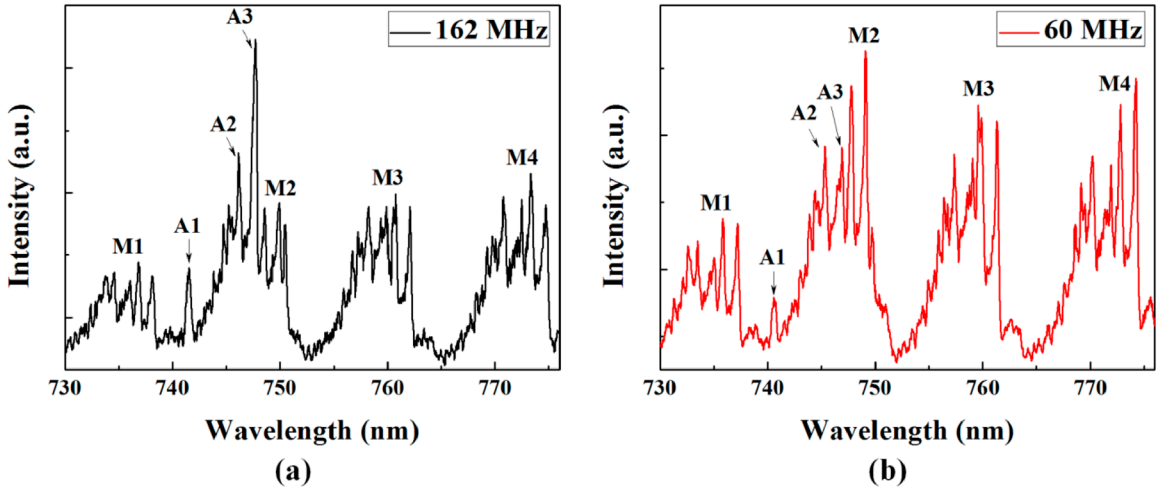

Figure 4. OES spectra of N_2 plasmas operated at 705 mW cm^{-2} and 50 mTorr for (a) the 162 MHz multi-tile push–pull source and (b) 60 MHz CCP source for the wavelength range from 730 to 776 nm.

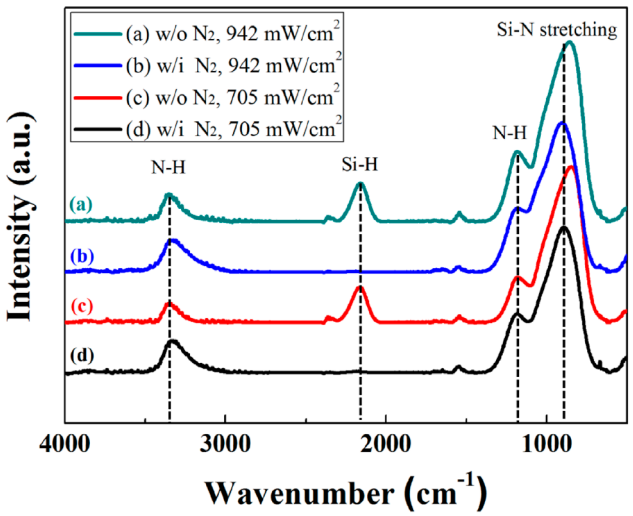

Figure 5. FTIR spectra measured for 300 nm thick SiN_x thin film deposited for different rf powers of 705–942 mW cm^{-2} and for the gas mixtures of $NH_3/SiH_4 = 3{:}1$ (without N_2) and $NH_3/SiH_4/N_2 = 3{:}1{:}4$ (with N_2).

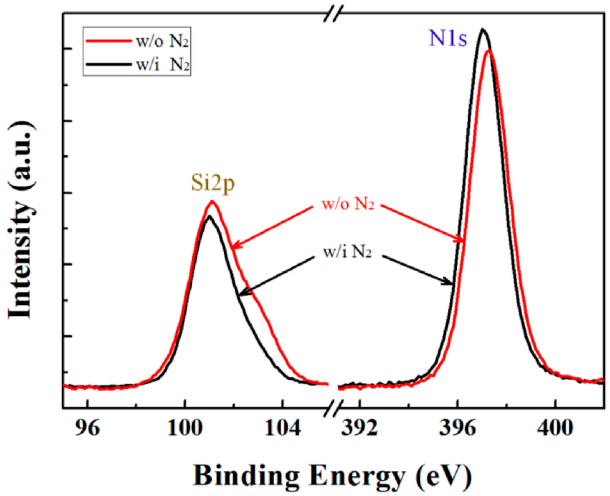

	w/i N_2		w/o N_2	
Atom	**Si**	**N**	**Si**	**N**
Percentage (%)	43.12	56.88	50.49	49.51

Figure 6. XPS narrow scan data (Si 2p at 101 eV and N 1s at 397 eV) and the atomic percentages (Si and N) in the 300 nm thick SiN_x thin film (ignoring hydrogen content in the film) with and without N_2, deposited using the 162 MHz multi-tile push–pull plasma source at 705 mW cm^{-2}, 50 mTorr ($NH_3/SiH_4 = 3{:}1$), and 100 °C.

In plasma processing, the vibrational temperature (T_v) has been related to the trapped energy/energy reservoir in the molecules, thereby enhancing the chemical reactivity of the molecules, while the rotational temperature has been related to the plasma thermometer [35]. Higher T_v can be beneficial in depositing high quality material at a lower substrate temperature; therefore, we expect that a high quality thin film can be deposited by the 162 MHz multi-tile push–pull plasma source, due to the high plasma density (n_e), low electron temperature (T_e), and higher vibrational temperature (T_v).

Using a 162 MHz multi-tile push–pull plasma source increased the nitrogen dissociation compared to the 60 MHz CCP source for the N_2 plasma. Figure 4 shows the OES spectra of N_2 plasmas operated at 705 mW cm^{-2} and 50 mTorr for (a) the 162 MHz multi push–pull source and (b) 60 MHz CCP source for the wavelength range from 730 to 776 nm. The optical emission peaks of multiple broad bands (M1–M4) are related to the first positive molecular transitions of N_2 and the three peaks (A1–A3) at 742.36 (3s $^4P_{1/2}$–3p ^4S transition), 744.23 (3s $^4P_{3/2}$–3p ^4S transition), and 746.83 nm (3s $^4P_{5/2}$–3p ^4S transition) are related to the atomic transition of N [38–40].

As shown in figures 4(a) and (b), the optical emission peak intensities of the multiple broad bands (M1–M4) were lower and those of the three atomic peaks (A1–A3) were higher for the 162 MHz multi-tile push–pull plasma source compared to the 60 MHz CCP source, indicating more significant dissociation of N_2 for the 162 MHz multi-tile push–pull plasma source than the 60 MHz CCP source. We believe that the higher N_2 dissociation characteristic of the 162 MHz multi-tile push–pull source helps in forming high quality SiN_x deposition

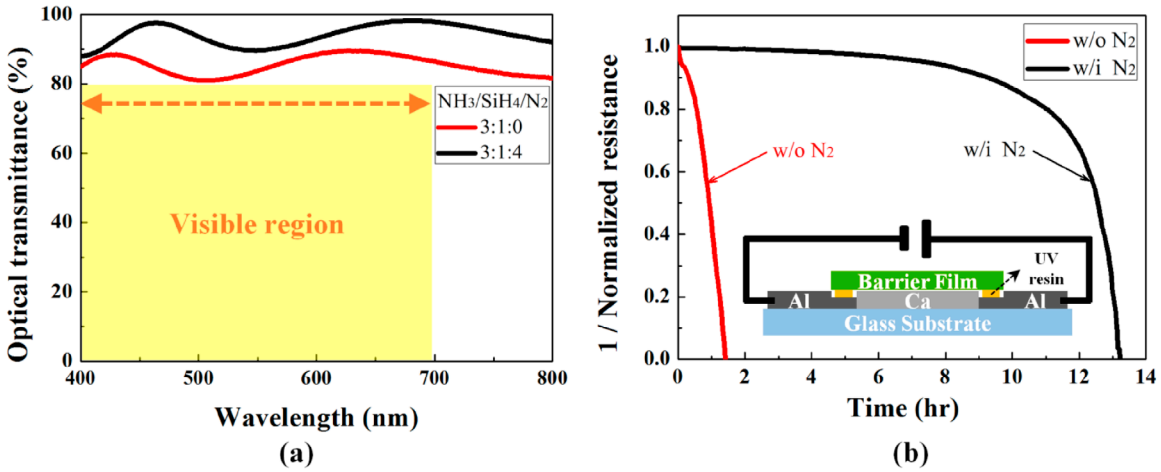

Figure 7. (a) Optical transmission percentages measured using UV–Vis–NIR spectroscopy, and (b) WVTR by the Ca test for 300 nm thick SiN_x thin films deposited on glass substrates with and without N_2. The deposition conditions were the same as those in figure 6. The Ca test was carried out at accelerating conditions of 85 °C and 85% RH.

when adding N_2 to the NH_3/SiH_4 plasma for the 162 MHz multi-tile push–pull plasma source.

Using the 162 MHz multi-tile push–pull plasma source, SiN_x thin films were deposited at 705–942 mW cm^{-2}, 50 mTorr, and 100 °C of substrate temperature (T_s). We used the gas mixtures of NH_3 (150 sccm)/SiH_4 (50 sccm) = 3:1 and NH_3 (150 sccm)/SiH_4 (50 sccm)/N_2 (200 sccm) = 3:1:4 to deposit SiN_x thin films on substrates; therefore, two different gas mixture conditions (with and without N_2) were used while the ratio of NH_3/SiH_4 was fixed (the ratio of NH_3/SiH_4 has been previously optimized before the N_2 addition). For these gas mixtures, the deposition rates of SiN_x were in the range of 75–80 nm min^{-1} for 705 mW cm^{-2} and 95–100 nm min^{-1} for 942 mW cm^{-2} and the qualities of these SiN_x thin films were investigated using FTIR. Figure 5 shows the FTIR spectra measured for 300 nm thick SiN_x thin films deposited for different rf power densities of 705–942 mW cm^{-2} and for gas mixtures of NH_3/SiH_4 = 3:1 (without N_2) and $NH_3/SiH_4/N_2$ = 3:1:4 (with N_2). For the wave number range of 500–4000 cm^{-1}, we observed absorption peaks related to N–H stretching (3338 cm^{-1} and 1186 cm^{-1}), Si–H stretching (2160 cm^{-1}), and Si–N stretching (891 cm^{-1}).

As shown in figure 5, the SiN_x thin films deposited without N_2 for both 705 and 942 mW cm^{-2} exhibited the absorption peak at 2160 cm^{-1} related to the Si–H bond, while the film deposited with N_2 for both powers exhibited imperceptibly low Si–H absorption peak intensity. The 162 MHz multi-tile push–pull plasma appears to change Si–H bonds to Si–N bonds on the deposited hydrogenated SiN_x film surface, due to the high atomic N concentration in the plasma (as shown in figure 4). The Si–H bonding in the hydrogenated SiN_x film increases the porosity in the film, increases the oxidation rate, and decreases the optical transmittance [2, 21]. Therefore, we believe a higher quality SiN_x can be deposited with the addition of N_2 for the 162 MHz multi-tile push–pull plasma. In addition, the absorption peak intensities related to N–H bonds at 3338 cm^{-1} and 1186 cm^{-1} were lower about 40.9 and 23.1%, respectively, while the wave number related to Si–N bond shifted lower from 891 cm^{-1} to 846 cm^{-1} for the SiN_x deposited without N_2 compared to that deposited with N_2. For more silicon-rich SiN_x film, previous investigations revealed that H-related peaks changed from N–H to Si–H, while the main Si–N peak shifted to a lower wave number [41]. Therefore, we believe that a more stoichiometric SiN_x film with less hydrogen content (close to Si_3N_4) can be obtained with the 162 MHz multi-tile push–pull plasma source using $NH_3/SiH_4/N_2$.

The SiN_x thin films deposited using the 162 MHz multi-tile push–pull plasma source (with and without N_2) were further investigated by XPS. Figure 6 shows the XPS narrow scan data (Si 2p at 101 eV and N 1s at 397 eV) and the atomic percentages (Si and N) in the 300 nm thick SiN_x thin film (ignoring hydrogen content in the film) with and without N_2, using the 162 MHz multi-tile push–pull plasma source at 705 mW cm^{-2}, 50 mTorr (NH_3/SiH_4 = 3:1), and 100 °C. As shown in figure 6, by using the $NH_3/SiH_4/N_2$ (w/i N_2) gas mixture instead of NH_3/SiH_4 (w/o N_2), the atomic percentages of N/Si changed from 49.51%/50.49% (=0.98) to 56.88%/43.12% (=1.32). Therefore, the deposited SiN_x film changed from the silicon rich SiN_x to near stoichiometric Si_3N_4 (=1.33) by using N_2 added to the NH_3/SiH_4 gas mixture.

For an application using the SiN_x thin film deposition as the thin film encapsulation layer, the SiN_x thin film needed to exhibit not only a high WVTR, but also high optical transmission. Figure 7 shows: (a) the optical transmission percentages measured using UV–Vis–NIR spectroscopy, and (b) the WVTR by the Ca test for 300 nm thick SiN_x thin films deposited on glass substrates (with and without N_2). The deposition conditions were the same as those in figure 6. For the Ca test, a Ca layer and Al electrodes were deposited on the glass substrates before the SiN_x thin film deposition, as shown in the inset of figure 7(b), for the estimation of WVTR by the increase of Ca resistance with time via the oxidation of Ca.

As shown in figure 7(a), SiN_x thin film deposited without N_2 exhibited an optical transmission percentage of a little higher than 80% for the visible wavelength range of 400–700 nm, possibly due to the Si–H bonding and high silicon percentage in the film. The SiN_x thin film deposited with

N_2 exhibited a transmittance percentage higher than 90%, sufficiently high for the thin film encapsulation layer due to the lack of Si–H bonding in the film and near stoichiometric Si_3N_4 composition. When the WVTR was estimated by the Ca test, shown in figure 7(b), the WVTR values of the SiN_x thin films deposited with and without N_2 were measured as 1.18×10^{-4} g $(m^2 \cdot d)^{-1}$ (very good WVTR for a single layer film) and 1.58×10^{-3} g $(m^2 \cdot d)^{-1}$ (good), respectively. Therefore, by using the 162 MHz multi-tile push–pull plasma source with N_2 added to NH_3/SiH_4 ($NH_3/SiH_4/N_2 = 3{:}1{:}4$), we could obtained a high quality SiN_x encapsulation layer having a high optical transmission percentage.

4. Conclusions

In this study, for the deposition of a SiN_x encapsulation layer, a VHF (162 MHz) multi-tile push–pull-type plasma source was used and the characteristics of the N_2 plasma and the SiN_x thin film deposited with and without N_2 added to NH_3/SiH_4 were investigated. We also compared the N_2 plasma characteristics of the 162 MHz multi-tile push–pull plasma source with those of a lower frequency (60 MHz) CCP source. The 162 MHz push–pull-type plasma showed a lower electron temperature, a higher vibrational temperature, and a higher N_2 dissociation compared to a lower frequency (60 MHz) CCP. When SiN_x thin films were deposited with a mixture of NH_3/SiH_4 (with and without N_2), a stoichiometric amorphous Si_3N_4 layer with very low Si–H bonding could be deposited for the gas mixture with N_2, while a silicon-rich SiN_x layer with high Si–H bonding could be deposited for the gas mixture without N_2. When the optical transmittance and the WVTR were measured with the 300 nm thick SiN_x deposited using the 162 MHz multi-tile push–pull plasma source with N_2 added NH_3/SiH_4, high optical transmittance (>90%) and a low WVTR (1.18×10^{-4} g $(m^2 \cdot d)^{-1}$) could be obtained at a substrate temperature of 100 °C. In addition, the VHF multi-tile push–pull plasma source showed significantly less standing wave problem (non-uniformity for large area processing being far more significant for general CCP sources operated at VHF). Therefore, we believe that the VHF multi-tile push–pull plasma source can be applicable to deposit high quality thin films, including a thin film encapsulation layer on large area substrates.

Acknowledgments

This research was supported by the Industry Technology R&D program of MOTIE/KEIT (10050501, Development of laser-assisted hybrid inorganic deposition system for flexible organic device passivation). This research was also supported by Samsung Electronics and the National Strategic Research Framework (NSRF) 2007–2013 funded by Enterprise Ireland CF20144043, co-funded by the European Regional Development Fund (ERDF)

References

[1] Park J, Chae H, Chung H K and Lee S I 2011 Thin film encapsulation for flexible AM-OLED: a review *Semicond. Sci. Technol.* **26** 034001
[2] Wuu D, Lo W, Chiang C, Lin H, Chang L, Horng R, Huang C and Gao Y 2005 Water and oxygen permeation of silicon nitride films prepared by plasma-enhanced chemical vapor deposition *Surf. Coat. Technol.* **198** 114–7
[3] Chen T, Wuu D, Wu C, Chiang C, Lin H, Chen Y and Horng R 2006 Effects of plasma pretreatment on silicon nitride barrier films on polycarbonate substrates *Thin Solid Films* **514** 188–92
[4] Gaugiran S, Gétin S, Fedeli J, Colas G, Fuchs A, Chatelain F and Dérouard J 2005 Optical manipulation of microparticles and cells on silicon nitride waveguides *Opt. Express* **13** 6956–63
[5] Milgram J, Wojcik J, Mascher P and Knights A 2007 Optically pumped Si nanocrystal emitter integrated with low loss silicon nitride waveguides *Opt. Express* **15** 14679–88
[6] Park S K, Oh J, Hwang C, Lee J, Yang Y S, Chu H Y and Kang K 2005 Ultra thin film encapsulation of OLED on plastic substrate *ETRI J.* **27** 545–50
[7] Carcia P, McLean R, Reilly M, Groner M and George S 2006 Ca test of Al_2O_3 gas diffusion barriers grown by atomic layer deposition on polymers *Appl. Phys. Lett.* **89** 031915
[8] Yang Y, Duan Y, Chen P, Sun F, Duan Y, Wang X and Yang D 2013 Realization of thin film encapsulation by atomic layer deposition of Al_2O_3 at low temperature *J. Phys. Chem.* C **117** 20308–12
[9] Majee S, Cerqueira M F, Tondelier D, Geffroy B, Bonnassieux Y, Alpuim P and Bourée J E 2015 Flexible organic–inorganic hybrid layer encapsulation for organic opto-electronic devices *Prog. Org. Coat.* **80** 27–32
[10] Kim T W, Yan M, Erlat A G, McConnelee P A, Pellow M, Deluca J, Feist T P, Duggal A R and Schaepkens M 2005 Transparent hybrid inorganic/organic barrier coatings for plastic organic light-emitting diode substrates *J. Vac. Sci. Technol.* A **23** 971–7
[11] Spee D, van der Werf K, Rath J and Schropp R 2012 Excellent organic/inorganic transparent thin film moisture barrier entirely made by hot wire CVD at 100 C *Phys. Status Solidi Rapid Res. Lett.* **6** 151–3
[12] Aberle A G 2001 Overview on SiN surface passivation of crystalline silicon solar cells *Sol. Energy Mater. Sol. Cells* **65** 239–48
[13] Huang W, Wang X, Sheng M, Xu L, Stubhan F, Luo L, Feng T, Wang X, Zhang F and Zou S 2003 Low temperature PECVD SiN*x* films applied in OLED packaging *Mater. Sci. Eng.* B **98** 248–54
[14] Mandlik P, Gartside J, Han L, Cheng I, Wagner S, Silvernail J A, Ma R, Hack M and Brown J J 2008 A single-layer permeation barrier for organic light-emitting displays *Appl. Phys. Lett.* **92** 103309
[15] Surendra M and Graves D 1991 Capacitively coupled glow discharges at frequencies above 13.56 MHz *Appl. Phys. Lett.* **59** 2091–3
[16] Kitamura T, Nakano N, Makabe T and Yamaguchi Y 1993 A computational investigation of the RF plasma structures and their production efficiency in the frequency range from HF to VHF *Plasma Sources Sci. Technol.* **2** 40
[17] Kitajima T, Takeo Y, Nakano N and Makabe T 1998 Effects of frequency on the two-dimensional structure of capacitively coupled plasma in Ar *J. Appl. Phys.* **84** 5928–36
[18] Matsuda A, Takai M, Nishimoto T and Kondo M 2003 Control of plasma chemistry for preparing highly stabilized

amorphous silicon at high growth rate *Sol. Energy Mater. Sol. Cells.* **78** 3–26
[19] Takeuchi Y, Nawata Y, Ogawa K, Serizawa A, Yamauchi Y and Murata M 2001 Preparation of large uniform amorphous silicon films by VHF-PECVD using a ladder-shaped antenna *Thin Solid Films* **386** 133–6
[20] Hebner G and Paterson A 2010 Ion temperature and velocity in a 300 mm diameter capacitively coupled plasma reactor driven at 13, 60 and 162 MHz *Plasma Sources Sci. Technol.* **19** 015020
[21] Takagi T, Takechi K, Nakagawa Y, Watabe Y and Nishida S 1998 High rate deposition of a-Si: H and a-SiN_x: H by VHF PECVD *Vacuum* **51** 751–5
[22] Kobayashi S, Ohrui N, Chao Y, Aoki T, Kobayashi H and Asakawa T 2007 Deposition of luminescent a-SiN_x: H Films with SiH_4–N_2 gas mixture by VHF–PECVD using novel impedance matching method *J. Mater. Sci. Mater. Electron.* **18** 29–32
[23] Lieberman M, Booth J, Chabert P, Rax J and Turner M 2002 Standing wave and skin effects in large-area, high-frequency capacitive discharges *Plasma Sources Sci. Technol.* **11** 283
[24] Sansonnens L, Schmidt H, Howling A, Hollenstein C, Ellert C and Buechel A 2006 Application of the shaped electrode technique to a large area rectangular capacitively coupled plasma reactor to suppress standing wave nonuniformity *J. Vac. Sci. Technol.* A **24** 1425–30
[25] Monaghan E 2014 VHF-PECVD and analysis of thin nano-crystalline silicon films with a multi-tile plasma source for solar energy applications *Doctoral Dissertation,* Dublin City University
[26] Klaus J, Ott A, Dillon A and George S 1998 Atomic layer controlled growth of Si_3 N_4 films using sequential surface reactions *Surf. Sci.* **418** L14–9
[27] Diebold A C 2001 *Handbook of Silicon Semiconductor Metrology* (CRC Press)
[28] Sze S M and Ng K K 2006 *Physics of Semiconductor Devices* (Wiley)
[29] Alpuim P, Gonçalves L, Marins E S, Viseu T, Ferdov S and Bourée J 2009 Deposition of silicon nitride thin films by hot-wire CVD at 100 C and 250 C *Thin Solid Films* **517** 3503–6
[30] Majee S, Cerqueira M, Tondelier D, Geffroy B, Bonnassieux Y, Alpuim P and Bourée J 2013 The effect of argon plasma treatment on the permeation barrier properties of silicon nitride layers *Surf. Coat. Technol.* **235** 361–6
[31] Britun N, Gaillard M, Ricard A, Kim Y, Kim K and Han J 2007 Determination of the vibrational, rotational and electron temperatures in N_2 and Ar–N_2 rf discharge *J. Phys. D: Appl. Phys.* **40** 1022
[32] Ricard A 1995 *Reactive Plasmas* (Paris: Société Française du Vide) p 156
[33] Lofthus A and Krupenie P H 1977 The spectrum of molecular nitrogen *J. Phys. Chem. Ref. Data* **6** 113–307
[34] Chen Z, Donnelly V M, Economou D J, Chen L, Funk M and Sundararajan R 2009 Measurement of electron temperatures and electron energy distribution functions in dual frequency capacitively coupled CF_4/O_2 plasmas using trace rare gases optical emission spectroscopy *J. Vac. Sci. Technol.* A **27** 1159–65
[35] Rehman N, Khan F, Khattak N and Zakaullah M 2008 Effect of neon mixing on vibrational temperature of molecular nitrogen plasma generated at 13.56 MHz *Phys. Lett.* A **372** 1462–8
[36] Masoud N, Martus K, Figus M and Becker K 2005 Rotational and vibrational temperature measurements in a high-pressure cylindrical dielectric barrier discharge (C-DBD) *Contrib. Plasma Phys.* **45** 32–9
[37] Van Veldhuizen E, Bisschops T, Van Vliembergen E and Van Wolput J 1985 Absolute densities of reaction products from plasma etching of quartz *J. Vac. Sci. Technol.* A **3** 2205–8
[38] McCullough R, Geddes J, Croucher J, Woolsey J, Higgins D, Schlapp M and Gilbody H 1996 Atomic nitrogen production in a high efficiency microwave plasma source *J. Vac. Sci. Technol.* A **14** 152–5
[39] Czerwiec T, Greer F and Graves D 2005 Nitrogen dissociation in a low pressure cylindrical ICP discharge studied by actinometry and mass spectrometry *J. Phys. D: Appl. Phys.* **38** 4278
[40] Ichikawa Y, Sakamoto T, Nezu A, Matsuura H and Akatsuka H 2010 Actinometry measurement of dissociation degrees of nitrogen and oxygen in N_2–O_2 microwave discharge plasma *Japan. J. Appl. Phys.* **49** 106101
[41] Vogt M and Hauptmann R 1995 Plasma-deposited passivation layers for moisture and water protection *Surf. Coat. Technol.* **74** 676–81